THE JOURNAL OF BIOLOGICAL CHEMISTRY
Vol. 276, No. 15, Issue of April 13, pp. 12249–12256, 2001
Printed in U.S.A.

Calcium-activated Potassium Channels Sustain Calcium Signaling in T Lymphocytes

SELECTIVE BLOCKERS AND MANIPULATED CHANNEL EXPRESSION LEVELS*

Received for publication, December 15, 2000
Published, JBC Papers in Press, January 22, 2001, DOI 10.1074/jbc.M011342200

Christopher M. Fanger‡§, Heiko Rauer¶, Amber L. Neben‡, Mark J. Miller‡, Heike Rauer‖, Heike Wulff‡, Joaquin Campos Rosa, C. Robin Ganellin**, K. George Chandy‡, and Michael D. Cahalan‡ ‡‡**

*From the ‡Department of Physiology and Biophysics, University of California, Irvine, California 92697-4561, ¶4SC AG Drug Discovery, 82152 Martinsried, Germany, ‖A. Bernauer Strasse, 80687 München, Germany, and the **Department of Chemistry, University College London, 20 Gordon Street, London WC1H OAJ, England*

To maintain Ca^{2+} entry during T lymphocyte activation, a balancing efflux of cations is necessary. Using three approaches, we demonstrate that this cation efflux is mediated by Ca^{2+}-activated K^+ (K_{Ca}) channels, h*SKCa2* in the human leukemic T cell line Jurkat and h*IKCa1* in mitogen-activated human T cells. First, several recently developed, selective and potent pharmacological inhibitors of K_{Ca} channels but not K_V channels reduce Ca^{2+} entry in Jurkat and in mitogen-activated human T cells. Second, dominant-negative suppression of the native K_{Ca} channel in Jurkat T cells by overexpression of a truncated fragment of the cloned *hSKCa2* channel decreases Ca^{2+} influx. Finally, introduction of the h*IKCa1* channel into Jurkat T cells maintains rapid Ca^{2+} entry despite pharmacological inhibition of the native small conductance K_{Ca} channel. Thus, K_{Ca} channels play a vital role in T cell Ca^{2+} signaling.

The human leukemic T cell line Jurkat is widely used as a model system to study intracellular signaling cascades during lymphocyte activation. These studies have revealed the critical requirement for two signaling pathways to complete lymphocyte activation. In the first pathway, activation of protein kinase C, particularly protein kinase Cθ, leads to the phosphorylation of several cytoplasmic proteins and the triggering of transcription via the assembly of the Fos/Jun transcription factor complex on AP1 elements in several genes (1–4). In the second cascade, the sustained entry of Ca^{2+} from the external milieu raises the cytoplasmic Ca^{2+} concentration, leading to gene transcription mediated by the nuclear factor of activated T cells (NF-AT)[1] (5, 6). Production of the key T cell cytokine IL-2 requires the simultaneous activation of both pathways, with Ca^{2+} being absolutely required for the process.

In human T lymphocytes and in Jurkat T cells, Ca^{2+} influx is mediated by the opening of voltage-independent Ca^{2+} release-activated Ca^{2+} (CRAC) channels (7–9). Movement of ions through open channels in the plasma membrane is driven by an electrochemical gradient. Upon T cell stimulation and opening of CRAC channels, the electrochemical gradient supporting Ca^{2+} entry is large, resulting in significant Ca^{2+} influx. However, Ca^{2+} entry could result in depolarization of the plasma membrane, limiting further influx. Therefore, to maintain Ca^{2+} entry over the time scale required for gene transcription, a balancing cation efflux is necessary. Efflux of K^+ ions through K^+ channels is thought to provide the electrochemical driving force for Ca^{2+} entry via regulation of membrane potential (10). We have directly tested this idea and identified the functionally important K^+ channel subtypes in Jurkat T cells and activated normal human T cells.

Jurkat T cells express two distinct K^+ channels. The first is a voltage-gated K^+ (K_V) channel encoded by the *Kv1.3* gene, and the second is a small conductance Ca^{2+}-activated K^+ (K_{Ca}) channel recently shown to be encoded by the h*SKCa2* gene (11–14). Human T cells possess a different K_{Ca} channel encoded by h*IKCa1*, in addition to *Kv1.3*, but do not express *SKCa2* (15–18). Earlier work investigating the roles of K^+ channels in lymphocyte activation was hampered by the lack of sufficiently specific blockers, leading to conflicting results and divergent interpretations (see, for example, Refs. 19 and 20). Expression levels of K_V and K_{Ca} channels are similar in Jurkat and in mitogen-activated human T cells, although the molecular identity of the K_{Ca} channel differs in these two cell types (15). This difference in expression pattern, the advent of new and highly specific blockers of all three channels, and the potential for genetic manipulation of functional expression levels provide an opportunity to examine the contributions of K^+ channels in regulating membrane potential and Ca^{2+} signaling in lymphocytes. Our results emphasize the importance of K_{Ca} channels in the modulation of Ca^{2+} signaling.

EXPERIMENTAL PROCEDURES

Cell Culture and Chemicals—Jurkat E6–1 and COS-7 cells were obtained from ATCC (Manassas, VA). Jurkat E6–1 cells were grown in RPMI medium supplemented with 10% fetal bovine serum, 2 mM glutamine, and 10 mM HEPES at densities of 1–9 $\times$ 10^5 in a 37 °C humidified incubator with 5% CO_2. COS-7 cells were cultured in Dulbecco's modified Eagle's medium containing 10% fetal calf serum and 2 mM glutamine and split twice weekly. Human T cells were isolated and cultured as described (21). T cells were preactivated by addition of 4 μg/ml

* This work was supported by National Institutes of Health Grants NS14609 and GM41514 (to M. D. C.), National Institutes of Health Grants MH59222 and GM54221 (to K. G. C.), a Feodor Lynen fellowship from the Alexander von Humboldt Foundation (to H. R.), and Deutsche Forschungsgemeinschaft Fellowship Grant WU 320/1-1 and Western States Affiliate of the American Heart Association Grant 9920014Y (to H. W.). The costs of publication of this article were defrayed in part by the payment of page charges. This article must therefore be hereby marked "*advertisement*" in accordance with 18 U.S.C. Section 1734 solely to indicate this fact.

§ Current address: AstraZeneca R & D Boston, 35 Gatehouse Dr., Waltham, MA 02451.

‡‡ To whom correspondence should be addressed. Tel.: 949-824-7776; Fax: 949-824-3143; E-mail: mcahalan@uci.edu.

[1] The abbreviations used are: NF-AT, nuclear factor of activated T cells; IL, interleukin; ChTX, charybdotoxin; CRAC, Ca^{2+} release-activated Ca^{2+}; Dap, diaminopropionic acid; GFP, green fluorescent protein; IKCa, intermediate conductance K_{Ca}; K_V, voltage-gated K^+; K_{Ca}, Ca^{2+}-activated K^+; SKCa, small conductance K_{Ca}; Tg, thapsigargin.

phytohemagglutinin or phorbol myristate acetate (33 nM) + ionomycin (1 μM) (Calbiochem) for 18–72 h prior to use. Unless otherwise specified, all reagents were obtained from Sigma and all optical filters from Chroma (Brattleboro, VT). The syntheses of bis-quinolinium cyclophane compounds UCL 1530 (8, 19-diaza-1,7(1,4)-diquinolina-3,5(1,4)-dibenzenacyclononadecanephanedium tetratrifluoroacetate hydrate), UCL 1684 (6, 10-diaza-1,5(1,4)-diquinolina-3(1,3),8(1,4)-dibenzenacyclodecaphanedium tritrifluoroacetate hydrate), UCL 1848 (8,14-diaza-1,7(1,4)-diquinolinacyclotetradecaphanedium ditrifluoroacetate), and UCL 2079 (8, 14-diaza-1,7(1,4)-di(6-trifluoromethylquinolina) cyclotetradecaphanedium ditrifluoroacetate) have been previously described (22–25). UCL 1684 is very stable in aqueous solution, showing no significant degradation after 24 h in culture medium at 37 °C (data not shown). The stability of other drugs was not tested over long periods of time. ShK-Dap[22] and ChTX-Glu[32] were obtained from BACHEM (King of Prussia, PA).

Transfection of Constructs into Mammalian Cells—In each electroporation cuvette (gap of 0.4 cm), 10^7 Jurkat cells and 10 μg of the DNA of interest were electroporated at 960 μF, 250 V, and then resuspended in 15 ml of fresh culture medium and returned to the incubator for 36–60 h prior to use. COS-7 cells (5×10^5 cells/chamber) were plated in culture chambers and transiently transfected using the Lipofectin transfection reagent (Life Technologies, Inc.) with the DNA of interest following the manufacturer's recommended protocol in OptiMEM medium (Life Technologies, Inc.). Following an 8–12-h transfection, the cells were placed in fresh growth medium in the incubator for 48 h. Typical transfection efficiencies using this protocol were 18–33%. The DNA vectors used for transfection were prepared using the Qiagen (Valencia, CA) endotoxin-free plasmid maxi-prep kit.

DNA Constructs—The N-terminal GFP fusion protein of human *IKCa1* (GFP-*IKCa1*) was a gift from J. Aiyar (AstraZeneca Pharmaceuticals, Wilmington, DE) and was generated by subcloning h*IKCa1* into the pEGFP-C1 vector (CLONTECH, Palo Alto, CA) as a *Bam*HI/*Bgl*II-Xho fragment. This cloning strategy introduced 12 extra amino acids between GFP and the initiation codon of *IKCa1*. The expressed sequence tag clone IMAGE: 2248 (GenBank™ accession number AI810558), corresponding to nucleotides 491–2193 of the *SKCa2* sequence AF239613, was isolated from the pT7T3 Pac Vector (Amersham Pharmacia Biotech) using *Not*I and *Eco*RI restriction sites and subcloned into pBluescript and from there into the *Sac*I restriction site of the pGFP-C1 expression vector. The truncated h*SKCa2* dominant negative construct was generated by removing a 1.24-kilobase pair *Bcl*I fragment from the GFP-*SKCa2* construct, leaving a 564-base pair insert encoding the h*SKCa2* N-terminal proximal region terminating in the S3 transmembrane domain. The human *SKCa3* clone (GenBank™ accession number AJ251016) containing 19 polyglutamines in the N terminus was cloned in frame to GFP in the GFP vector as an *Eco*RI/*Bam*I fragment. HEK-293 cells expressing the skeletal muscle sodium channel *hSKM1* (SCN4A) were a gift from Dr. F. Lehmann-Horn (University of Ulm, Germany) (26). The murine *Kv1.3* channel is stably expressed in L929 cells as previously described (12). The *hSlo* construct was the gift of Dr. Ligia Toro (University of California, Los Angeles, CA) and is expressed following injection into *Xenopus* oocytes (27, 28).

Patch Clamp Experiments—For all K_{Ca} experiments, electrophysiological recordings were made in the whole-cell mode with a holding potential of −40 mV and an internal solution consisting of 130 mM potassium aspartate, 10 mM K_2EGTA, 8.55 mM $CaCl_2$, 2.08 mM $MgCl_2$, and 10 mM HEPES, pH 7.2, with a calculated free [Ca^{2+}] of ~1 μM. In K_V experiments, whole-cell recordings were made with a holding potential of −80 mV and an internal solution identical except that it contained 2.28 mM $CaCl_2$, resulting in a calculated free [Ca^{2+}] of ~50 nM. K_V experiments also used a leak subtraction regimen in which the leak pulse was applied after each voltage pulse. External solutions consisted of normal Ringer solution (155 mM NaCl, 4.5 mM KCl, 2 mM $CaCl_2$, 1 mM $MgCl_2$, 10 mM D-glucose, and 5 mM HEPES, pH 7.4), K^+ Ringer solution (with identical ingredients except that all NaCl was substituted by KCl, resulting in a final KCl concentration of 159.5 mM), or 40 mM K^+ Ringer solution, in which these two solutions were mixed to yield a final Na^+ concentration of 119.5 mM and a final K^+ concentration of 40 mM. Whole-cell patch clamp recordings were performed using the equipment and techniques described previously, and all data were corrected for a liquid junction potential of −13mV for aspartate-based solutions (29).

Cytokine Expression Assays—Jurkat cells were stimulated as described above for T cells but in 96-well tissue culture plates with 10^5 cells in 200 μl of growth medium. Cytokine production was assayed using the OptEIA enzyme-linked immunosorbent assay kit (BD-Pharmingen, San Diego, CA) and a fluorescence plate reader (Molecular Devices, Sunnyvale, CA) to quantify production of IL-2 and IL-8.

Confocal Microscopy—Confocal fluorescence images were taken with a Bio-Rad MRC-600 equipped with an argon laser (488 nm) and a fluorescein isothiocyanate filter set (500–530 nm). All images were acquired under a 63× oil objective on a Zeiss Axiovert 35 microscope. Z-series sections were captured at 0.5-μm intervals, and optical section thickness was estimated to be ~0.45-μm.

Ca^{2+} Imaging and Membrane Potential Measurements—Cells were loaded in 1 μM fura-2/AM ester (Molecular Probes, Eugene, OR) at 21–24 °C for 30 min, washed, and stored in the dark until use (within 3 h). Intracellular Ca^{2+} concentrations were estimated, and experiments were performed utilizing a complete video microscopic, ratiometric Ca^{2+} imaging system (Videoprobe, ETM Systems), as previously described (30). At the beginning of data collection, the extracellular solution was normal Ringer solution. Store depletion in the presence of Tg required perfusion with a 0-Ca^{2+} version of normal Ringer solution in which $CaCl_2$ was replaced by additional $MgCl_2$ to keep divalent concentrations constant and in which 1 mM EGTA was used to chelate residual Ca^{2+}. During measurements on transfected cells, individual GFP-positive, and thus successfully transfected, cells were identified and marked for analysis using a fluorescein isothiocyanate filter set consisting of a 480 ± 20 nm exciter, 505 nm dichroic mirror, and 520 nm long-pass emission filter. By comparing Ca^{2+} responses of GFP-*hSKCa2*Δ-expressing or GFP-*hIKCa1*-expressing cells with GFP-expressing vector control cells, we eliminated the risk of inaccurate quantification due to small amounts of contamination of the fura-2 signal by GFP fluorescence bleed-through. Data processing and statistical analysis were carried out using IgorPRO (Wavemetrics, Lake Oswego, OR) and Excel (Microsoft, Redmond, WA) software. The bis-oxonol dye bis-(1, 3-dibutylbarbituric acid)trimethine oxonol (DiBAC4(3), Molecular Probes) was used as an indicator of membrane potential in imaging experiments using the same software and hardware described for Ca^{2+} imaging, and using the fluorescein, filter set described above. Cells were preequilibrated with 125 nM DiBAC4(3) for 5–10 min prior to the start of each experiment, and dye concentration was maintained in all external solutions throughout the experiment.

RESULTS

Specific K^+ Channel Blockers Define the Role of K_V and K_{Ca} Channels in Jurkat Ca^{2+} Signaling—Using the patch clamp technique, we characterized highly potent and specific K_{Ca} and K_V channel blockers in Jurkat T cells and activated human T lymphocytes. In Jurkat cells, whole-cell recording with Ca^{2+} maintained at a low concentration inside the pipette revealed only K_V currents (Fig. 1*A*). These currents inactivated during repetitive pulsing and were blocked by ShK-Dap[22], a sea anemone peptide modified to gain specificity for the *Kv1.3* channel (IC_{50} = ~25 pM) (31). Application of 10 nM ShK-Dap[22] blocked ~97% of the K_V current. The voltage dependence, inactivation kinetics, and pharmacological properties of Jurkat K_V currents are consistent with *Kv1.3* encoding this channel, as reported previously (32).

Elevation of [Ca^{2+}] inside the pipette to 1 μM activated an additional small, voltage-independent current. By increasing extracellular K^+ concentrations to 40 mM, the inward component of this current could be observed. The current reversed near the predicted Nernst potential for a K^+-selective current in 40 mM K^+ extracellular solution (Fig. 1*B*). Application of 10 nM apamin, a peptide from bee venom, completely and irreversibly blocked this K_{Ca} current (data not shown), in agreement with a previous study (11), whereas *Kv1.3* blockers ShK-Dap[22] (250 nM, Fig. 1*B*) and charybdotoxin (10 nM, data not shown) had little or no effect. Recently, a group of bis-quinolinium derivatives developed by the group of C. R. Ganellin and D. H. Jenkinson at University College London were found to block with high affinity the apamin-sensitive small conductance K_{Ca} channel in rat superior cervical ganglion cells (33). We tested these same compounds on the apamin-sensitive K_{Ca} current in Jurkat T cells. The bis-quinolinium cyclophane UCL 1684 (see under "Experimental Procedures" for full name) at a concentration of 10 nM blocked 95 ± 5% of the K_{Ca} current but had no effect on the K_V current even at 250 nM (Fig. 1, *A* and *B*). Blocking was rapid (usually complete within 1 min) and, in contrast to apamin, rapidly reversible. The dose-response curve

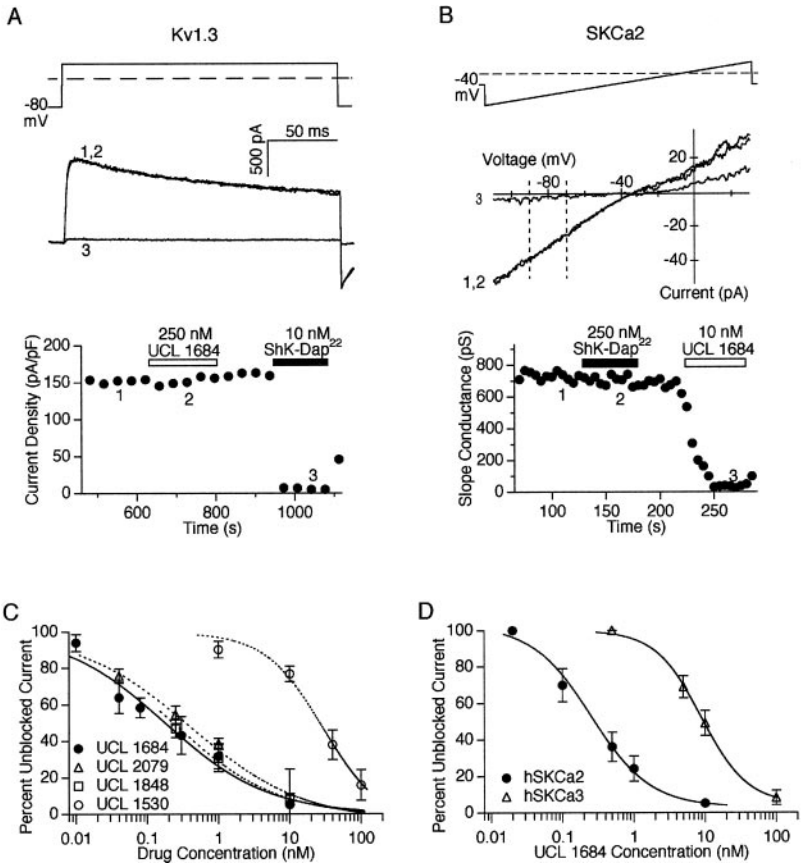

FIG. 1. **Selective K^+ channel blockers.** Whole-cell recordings in the presence of 40 mM K^+-containing extracellular Ringer solution to amplify inward K^+ currents. *A,* Jurkat T cells dialyzed with low Ca^{2+} internal solution. Current densities (peak current from each voltage step divided by cell capacitance, *bottom*) and raw data from individual steps (*middle*) are shown. Repeated stimuli at 35-s intervals using the protocol shown (*top*) elicited voltage-gated K^+ currents (*1*) that were not affected by 250 nM UCL 1684 (*2*) but were completely blocked by 10 nM ShK-Dap^{22} (*3*). K_V data are shown after leak subtraction as described under "Experimental Procedures." *B,* K_{Ca} current was observed in isolation by whole-cell recording from a Jurkat T cell dialyzed with 1 μM Ca^{2+} during measurement of slope conductance at ~−80 mV (*dashed lines* denote region of measurement). Ramp protocol (*top*) evoked Ca^{2+}-activated K^+ currents (*middle* and *bottom, 1*) that were unaffected by 250 nM ShK-Dap^{22} (*2*) but completely blocked by 10 nM UCL 1684 (*3*). Frequent pulses (every 10 s) and depolarized holding potentials (−40 mV) led to inactivation of K_V currents. *C* and *D,* dose-response curves for inhibition of Jurkat or cloned K_{Ca} channels by bis-quinolinium cyclophanes. Each *point* shown is the mean percentage of unblocked current of 3–5 cells at a given drug dose ± S.E. *Lines* illustrate fits to the Hill equation. K_{Ca} current, measured as the slope conductance at ~−80 mV, was compared before and after addition of the blockers shown to determine percent unblocked current. *C,* measurements of efficacy of block of all 4 UCL compounds on Jurkat K_{Ca} currents. *D,* effect of UCL 1684 in blocking the cloned channels h*SKCa2* and h*SKCa3*.

in Fig. 1*D* shows that UCL 1684 blocks the Jurkat K_{Ca} channel with subnanomolar affinity (IC_{50} = 180 pM), making it the most potent inhibitor of this channel yet described. The molecular identity of the K_{Ca} channel in Jurkat T cells was verified by measuring the efficacy of UCL 1684 in blocking current through the cloned human *SKCa*2 and *SKCa3* channels expressed in COS-7 cells (IC_{50} values of 280 pM and 9.5 nM, respectively). UCL 1684 selectively blocks Jurkat K_{Ca} channels and *SKCa2* channels over the closely related *SKCa3* channel and several other more distantly related channels (Fig. 1*D*; Table I). Other bis-quinolinium cyclophanes (UCL 2079, UCL 1848, and UCL 1530; see under "Experimental Procedures" for full names) also blocked Jurkat K_{Ca} currents with high affinity (Fig. 1*C*). Table I summarizes the selectivity of all compounds and demonstrates that UCL 1684, UCL 1848, and UCL 2079 are all ~10^4-fold more effective at blocking SKCa currents than any other channels tested. Because these drugs are highly specific for the K_{Ca} channel found in Jurkat T cells and appear equally potent in blocking the expressed human *SKCa2* channel, our results provide a confirmation that the *SKCa2* gene encodes the K_{Ca} channel in Jurkat T cells (13, 14).

We used a pharmacological approach to discern the contributions of *Kv1.3* and *SKCa2* channels to calcium signaling in Jurkat T-cells. Ca^{2+} signaling can be induced by thapsigargin (Tg), a specific inhibitor of the sarco-endoplasmic reticulum Ca^{2+} ATPase that enables study of Ca^{2+} entry independent of Ca^{2+} release from internal stores (34). Depletion of intracellular Ca^{2+} stores with Tg in the absence of extracellular Ca^{2+} activates CRAC channels in the plasma membrane, permitting Ca^{2+} entry upon reintroduction (35). In Jurkat T cells, the K_{Ca} channel inhibitor UCL 1684 reduced Ca^{2+} influx, but not the Tg-induced release of intracellular Ca^{2+} stores (Fig. 2*A*), in a dose-dependent manner that closely paralleled the dose-dependent block of the native K_{Ca} current (Fig. 2*B*). Maximal inhibition of the $[Ca^{2+}]_i$ plateau was achieved at 10 nM UCL 1684, a dosage that blocked 95 ± 5% of Jurkat K_{Ca} channels. This dosage of UCL 1684 had no effect on IL-2 production in Jurkat cells but inhibited IL-8 production by 30% (data not shown). In contrast, application of the *Kv1.3* blocker ShK-Dap^{22} (up to 10 nM) did not affect the Ca^{2+} response or cytokine production (Fig. 2*A* and data not shown). These results demonstrate that K_{Ca} channels but not K_V channels help maintain Jurkat cell Ca^{2+} entry.

The most likely mechanism by which UCL 1684 inhibits Ca^{2+} entry is depolarization of the membrane potential resulting from Ca^{2+} entry through CRAC channels in the absence of K_{Ca} channel function. To test this possibility, the membrane potential of Jurkat T cells was monitored using a voltage-sensitive dye during the same Tg stimulation protocol used in Fig. 2*A*. Treatment with Tg in the absence of extracellular Ca^{2+}

TABLE I
Ion channel selectivity of UCL drugs

IC_{50} values (in nM) of bis-quinolinium cyclophane derivatives were determined using whole cell recordings from cell lines expressing native or transfected ion channels. h*SKCa2* and h*SKCa3* are the human *SKCa2* and *SKCa3* genes, respectively, transiently expressed in COS-7 cells. m*Kv1.3* is the mouse lymphocyte voltage-gated K^+ channel stably expressed in L929 cells (12). h*Slo* is the large-conductance human K_{Ca} channel, and *hskm1* is a human skeletal muscle Na^+ channel (see under "Experimental Procedures"). IC_{50} values for drugs were estimated based on fits to the Hill equation. ND, not determined.

	Jurkat SK_{Ca}	h*SKCa2*	h*SKCa3*	m*Kv1.3*	T-cell h*IKCa1*	h*Slo* (maxiK)	h*skm1* (Na^+ channel)
UCL 1684	0.18	0.28	9.5	4900	>5000	>5000	>5000
UCL 1530	30	ND	ND	2100	4700	ND	ND
UCL 1848	0.24	ND	ND	ND	ND	ND	ND
UCL 2079	0.35	ND	ND	>5000	>5000	ND	ND

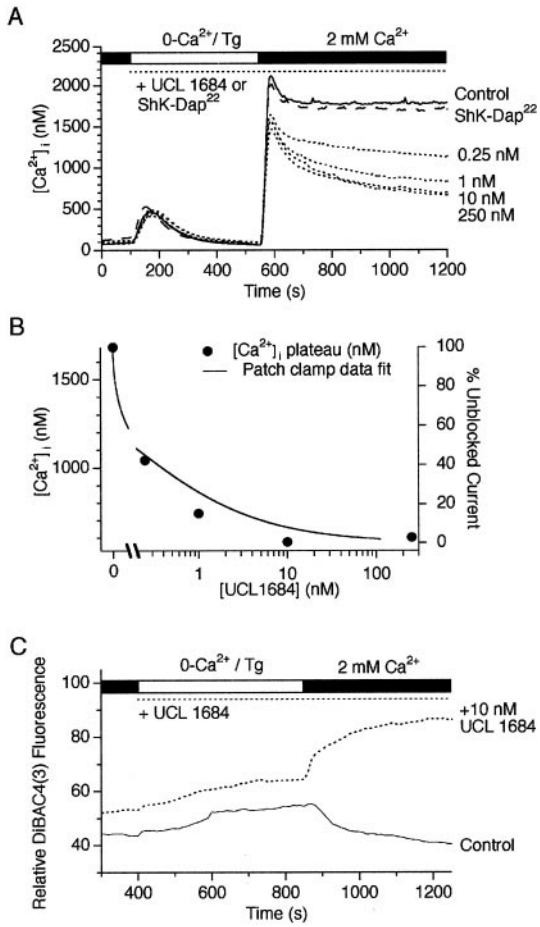

FIG. 2. **K_{Ca} (*SKCa2*) but not K_V block reduces Ca^{2+} influx in Jurkat T cells.** In Ca^{2+} imaging experiments, fura-2-loaded Jurkat cells and human T cells were stimulated with 1 μM Tg in 0-Ca^{2+} Ringer solution (see *bars* above panels) in the presence or absence of UCL 1684 or ShK-Dap^{22}. After ~8 min, normal Ringer solution (2 mM Ca^{2+}) was reintroduced, causing a rapid, sustained Ca^{2+} influx. *A,* Ca^{2+} responses of Jurkat cells stimulated with Tg in the presence of varying doses of UCL 1684 (*numbers*), of 10 nM ShK-Dap^{22}, or no drug (*control*). Each *trace* represents the average response of ~100 cells from a typical experiment. Combined addition of ShK-Dap^{22} and UCL 1684 had little or no added effect. *B,* comparison of the dose-response curve from patch clamp experiments shown in Fig. 1*C* (*solid line*) with the plateau Ca^{2+} values from *A* (*filled circles*). *C,* membrane potential was monitored during stimulation in the presence (*dotted trace*, 64 cells) or in the absence (*solid trace*, 45 cells) of UCL 1684 (10 nM). Increasing DiBAC4(3) fluorescence intensity indicates depolarization of the membrane potential. Tg (1 μM) was used in a stimulation protocol identical to that used in *A*.

caused a moderate depolarization of most cells, followed by a marked hyperpolarization upon Ca^{2+} readdition (Fig. 2*C, solid line*). This hyperpolarization must be caused by the opening of *SKCa2* channels because cells treated with UCL 1684 instead showed profound membrane depolarization following Ca^{2+} reintroduction (Fig. 2*C, dotted line*). Similar results were observed in perforated-patch current clamp recordings (data not shown). These results demonstrate the tight link between K_{Ca} channel opening, modulation of membrane potential, and regulation of Ca^{2+} entry.

The Role of K_{Ca} Channels in Activated Normal Human T Cells—Activated human T cells present an excellent system to further test the role of K_{Ca} channels in Ca^{2+} regulation. Mitogen-activated human T cells and Jurkat cells express similar numbers of K_V and K_{Ca} channels, suggesting that they may regulate calcium signaling in a similar manner. The K_V channel in human lymphocytes and in Jurkat T cells is encoded by the *Kv1.3* gene (32, 36). However, the K_{Ca} channel in human T cells is the product of the *IKCa1* gene that is phylogenetically related to the *SKCa2* gene found in Jurkat cells. Both K_{Ca} channels share a common calmodulin-dependent mechanism for calcium-dependent gating (29, 37, 38), and both exhibit a conserved genomic organization (39).

To test whether *IKCa1* and *SKCa2* serve similar functions in sustaining Ca^{2+} signaling, we used agents that are selective for the block of the K_{Ca} channels found in mitogen-activated human T cells, including the charybdotoxin mutant ChTX-Glu^{32} and the clotrimazole analogue TRAM-34 (28, 40). We first verified that these blockers are selective for *IKCa1* by testing them on this channel in an expressed system. As shown in Fig. 3*A, IKCa1* channels are blocked by ChTX-Glu^{32} (IC_{50} = ~30 nM) (28). Neither the UCL compounds (10 nM) nor ShK-Dap^{22} (250 nM) affected the *IKCa1* channel (Fig. 3*A* and data not shown). The triarylmethane blocker of *IKCa1*, TRAM-34 (IC_{50} = ~20 nM), also blocks native or expressed *IKCa1* current with high selectivity (data not shown) (40).

Tg-induced Ca^{2+} responses in human T cells activated for 48 h with anti-CD3 antibody are partially suppressed by the *IKCa1*-specific inhibitors ChTX-Glu^{32} and TRAM-34, as shown in Fig. 3*B,* whereas UCL 1684 (10 nM, Fig. 3*C*) had little effect. Note that the absence of any effect of UCL 1684 on Ca^{2+} influx in T cells argues that CRAC channels, too, are unaffected by this drug, because CRAC currents in human T cells and Jurkat cells are identical (8, 9). In parallel with the inhibition of Ca^{2+} influx in activated T lymphocytes achieved by the *IKCa1* blockers, TRAM-34 was previously reported to suppress proliferation of activated T-cells far more effectively than resting T cells (39, 40). In contrast, the *Kv1.3* blocker ShK-Dap^{22} (500 nM, Fig. 3*D*) did not inhibit Ca^{2+} influx in activated T cells (Fig. 3*D*), consistent with an earlier report that *Kv1.3* blockade does not suppress proliferation of activated cells (39). Taken together with the data on Jurkat cells, these results further emphasize the role of K_{Ca} channels in cells of the immune system.

Dominant-negative Knockout Strategy—To verify that UCL 1684 reduces Ca^{2+} entry in Jurkat cells by specific inhibition of the K_{Ca} channel, we used a dominant-negative suppression strategy to prevent K_{Ca} expression. A functional Jurkat K_{Ca} channel is expected to be a homotetramer of the SKCa2 protein. In K_V channels, tetramerization is partly determined by the

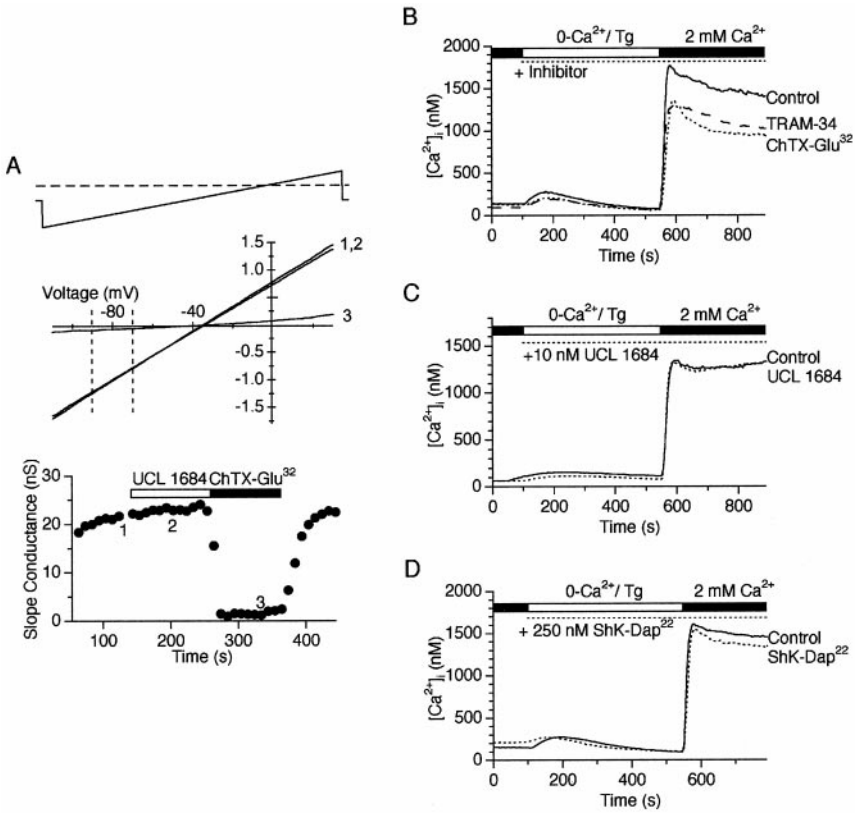

FIG. 3. **K_{Ca} (*IKCa1*) but not K_V block reduces Ca^{2+} influx in preactivated human T cells.** *A,* whole-cell K_{Ca} currents recorded from *IKCa1*-transfected Jurkat cells with 1 μM Ca^{2+} internal solution and 40 mM extracellular K^+ Ringer (*1*). These currents could be blocked by ChTX-Glu^{32} (1 μM, *3*) but not UCL 1684 (10 nM, *2*). The depolarized holding potential and rapidity of pulses caused inactivation of the native K_V current. *B,* in preactivated human T cells, depletion of intracellular Ca^{2+} stores with Tg and 0-Ca^{2+} followed by Ca^{2+} reintroduction resulted in sustained Ca^{2+} entry (*solid line*), just as it did in Jurkat cells. Blockade of the intermediate conductance K_{Ca} channel with 1 μM ChTX-Glu^{32} (*dotted line*) or 1 μM TRAM-34 (*dashed line*) reduces this Ca^{2+} entry. Shown are 97 control cells, 108 cells treated with ChTX-Glu^{32}, and 79 cells treated with TRAM-34. *C,* the mean Ca^{2+} response of 284 preactivated human T cells treated with both Tg and UCL 1684 (10 nM, *dotted line*) was indistinguishable from that of 281 preactivated Tg-treated control T cells (*solid line*). *D,* Ca^{2+} influx in preactivated, untreated human T cells (*solid trace*) was not significantly different from influx in preactivated T cells treated with the K_V blocker ShK-Dap^{22} (250 nM, *dotted trace*). Mean Ca^{2+} responses of 92 control cells and 81 cells treated with ShK-Dap^{22} are shown.

N-terminal T1 domain, and overexpression of N-terminal fragments containing the T1 domain results in dominant-negative suppression of native channels via co-assembly of the truncated fragments with native subunits in nonfunctional tetramers (41). Hypothesizing that the N termini of K_{Ca} channels contain a similar tetramerization domain, we transfected COS-7 cells and Jurkat T-cells with a GFP-tagged N-terminal fragment of the human SKCa2 gene (GFP-hSKCa2Δ). Confocal microscopy of transfected COS-7 cells revealed mainly endoplasmic reticulum localization of GFP-hSKCa2Δ (Fig. 4*A*); similar results were obtained with the smaller Jurkat cells (data not shown). Parallel patch clamp experiments were performed in control-transfected and GFP-hSKCa2Δ-transfected Jurkat cells. Expression of the GFP-hSKCa2Δ construct abolished whole-cell K_{Ca} current in Jurkat cells (Fig. 4*C*), compared with vector-transfected control cells (Fig. 4*B*). Interestingly, the hSKCa3 N-terminal fragment also suppressed this current (data not shown), suggesting that these two channels can heteromultimerize, as has been reported for SKCa2 and SKCa1 (42). These results strongly suggest that SKCa channels, like K_V channels, contain a tetramerization domain in the N terminus. The GFP-hSKCa2Δ cells were used to test the role of the K_{Ca} channel in Ca^{2+} signaling. Cells expressing the dominant-negative GFP-hSKCa2Δ construct exhibited significantly attenuated Ca^{2+} entry (Fig. 4*D, dotted line*) compared with vector-control cells, reinforcing the conclusion that functional activity of the K_{Ca} channel sustains normal Ca^{2+} signals in Jurkat cells. The decreased level of Tg-induced store release in cells expressing the GFP-hSKCa2Δ construct could in principle result from inhibited release of Ca^{2+} stores or from a smaller total store content. By perfusing ionomycin (4 μM) following depletion of stores with Tg, we found that GFP-hSKCa2Δ-expressing cells have a larger Tg-nonreleasable store content than vector-control cells (data not shown), suggesting that functional hSKCa2 could be related to store release in an unknown manner.

Recently, it was observed that treatment with the mitogenic lectin phytohemagglutinin decreases the number of *SKCa2* channels expressed in Jurkat cells (14). Corresponding to this decrease, we find that Tg-induced Ca^{2+} influx is reduced by ~50% in Jurkat cells activated with phytohemagglutinin for 48 h (data not shown), consistent with the suppression of Ca^{2+} signaling by pharmacological blockade of K_{Ca} channels (Figs. 2 and 3) and by knocking out native *SKCa2* expression using a dominant-negative construct (Fig. 4).

Compensation with a UCL 1684-resistant K_{Ca} Channel, IKCa1—We next tested whether the UCL 1684-resistant intermediate conductance K_{Ca} channel, h*IKCa1,* present in activated human T cells, can effectively substitute for the Jurkat *SKCa2* channel. Transfection with GFP-tagged h*IKCa1* (GFP-h*IKCa1*) led to endoplasmic reticulum and plasma membrane staining of COS-7 and Jurkat cells (Fig. 5*A*) and conferred expression of large K_{Ca} currents in both cell types (data not shown). Jurkat cells transfected with *IKCa1* expressed whole-cell K_{Ca} currents >100 times larger than those observed in cells transfected with vector alone (Fig. 5*B*). These currents were Ca^{2+}-activated, insensitive to UCL 1684, and blocked by

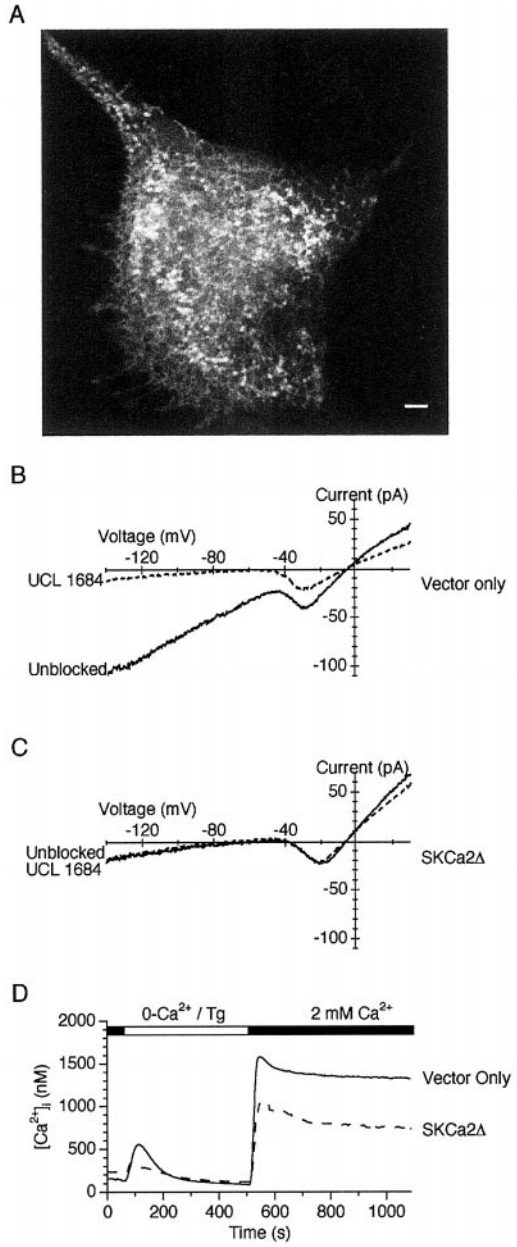

FIG. 4. **Dominant-negative suppression of *SKCa2* expression in Jurkat T cells results in a decreased Ca^{2+} response.** Jurkat cells and COS-7 cells were transfected with an otherwise empty vector conferring expression of GFP (vector control) or with a vector conferring expression of the N-terminal cytosolic fragment of h*SKCa2* conjugated to GFP (GFP-*hSKCa2*Δ). *A,* confocal microscopic image of COS-7 cells transfected with GFP-*hSKCa2*Δ. *Scale bar,* 1 μm. *B,* whole-cell recordings from Jurkat cells dialyzed with 1 μM Ca^{2+} internal solution. Control-transfected Jurkat cells with K^+ Ringer solution outside show sizable K_{Ca} currents (*solid line*) blockable by 10 nM UCL 1684 (*dashed line*). *C,* conversely, expression of GFP-*hSKCa2*Δ significantly suppressed K_{Ca} currents, leaving little current (*solid line*) that was blockable by UCL 1684 (*dashed line*). Mean current in GFP-*hSKCa2*Δ-expressing cells was ~30% of that observed in control cells (n = 6 GFP-*hSKCa2*Δ cells: mean slope conductance, 0.15 ± 0.02 nS; n = 7 control cells: mean slope conductance, 0.55 ± 0.08 nS; p = 0.01). *D,* Ca^{2+} responses of 20 Jurkat cells transfected with GFP-*hSKCa2*Δ (*dashed line*) and of 88 vector control Jurkat cells (*solid line*) in a protocol otherwise identical to that shown in Fig. 2*A*.

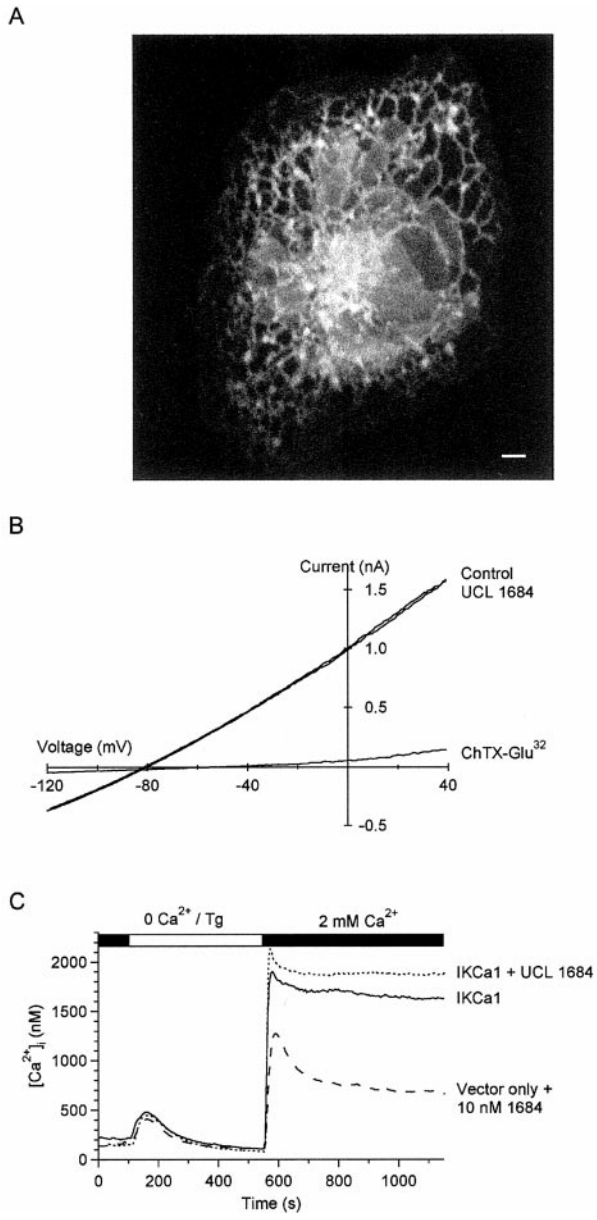

FIG. 5. **The h*IKCa1* channel found in human T cells can substitute effectively for the *SKCa2* channel found in Jurkat T cells.** COS-7 and Jurkat T cells were transiently transfected with GFP-*IKCa1* or with an otherwise empty vector conferring expression of GFP (vector control). *A,* confocal microscopic image of COS-7 cells transfected with GFP-*IKCa1*. *Scale bar,* 1 μm. *B,* in whole-cell recordings from Jurkat T cells with normal Ringer solution outside and 1 μM Ca^{2+} internal solution, transient transfection of GFP-*IKCa1* conferred expression of large K_{Ca} currents that were blocked by 1 μM ChTX-Glu^{32} but not by 10 nM UCL 1684. Mean current in GFP-*IKCa1*-transfected cells was 25.7 ± 8.9 nS, compared with 0.23 ± 0.04 nS in control cells (n = 11 GFP-*IKCa1* cells, n = 6 vector control cells). *C,* transient transfection with the h*IKCa1* channel rescues Jurkat cells from suppression of the Ca^{2+} response by UCL 1684 (10 nM). Traces shown are 41 GFP-h*IKCa1*-transfected control cells (*solid line*, three experiments), 60 GFP-h*IKCa1*-transfected cells treated with UCL 1684 (*dotted line*, five experiments), and 65 vector control cells treated with UCL 1684 (*dashed line*, three experiments).

the *IKCa1*-selective peptide ChTX-Glu^{32} (Fig. 5*B*) (28), demonstrating that the overexpressed GFP-tagged h*IKCa1* channel functions as expected. Cells overexpressing h*IKCa1* were rescued from pharmacological inhibition of Ca^{2+} influx by UCL 1684 (Fig. 5*C*). Thus, the h*IKCa1* channel can substitute for the native *SKCa2* channel in Jurkat cells and effectively sustains the Ca^{2+} response.

DISCUSSION

Using three independent strategies, we demonstrate a critical role for K_{Ca} channels, but not K_V channels, in regulating the Ca^{2+} signaling response in T lymphocytes. First, we used se-

lective and potent blockers of K_V and K_{Ca} channels provided by a series of bis-quinolinium compounds, a modified peptide from sea anemone toxin, and a scorpion toxin mutant peptide to inhibit *SKCa2*, *Kv1.3* and *IKCa1*, respectively. In Jurkat T cells, the bis-quinolinium cyclophane UCL 1684 inhibited Ca^{2+} influx with a potency that mirrored its dose-response curve for block of *SKCa2* current (Figs. 1 and 2 and Table I), whereas selective blockade of *Kv1.3* had little or no effect. Furthermore, in activated T cells, blockade of the native *IKCa1* channel with the selective and potent inhibitors, ChTX-Glu[32] and TRAM-34, significantly suppressed Ca^{2+} influx, whereas UCL 1684 had no effect in these cells, and *Kv1.3* blockers again were ineffective (Fig. 3). Second, dominant negative suppression of *SKCa2* channel expression in Jurkat cells effectively inhibited Ca^{2+} entry, confirming the functional importance of these channels by a completely independent experimental approach (Fig. 4). Third, overexpression of the pharmacologically distinct K_{Ca} channel, h*IKCa1,* in Jurkat T cells rescued Ca^{2+} entry from inhibition by UCL 1684 (Fig. 5). Thus, using a pharmacological strategy based on selective blockade of each channel in conjunction with molecular approaches to vary expression levels, we demonstrate that the *SKCa2* channel in Jurkat T cells and the *IKCa1* channel in human T cells sustain Ca^{2+} signaling.

Antigen-dependent activation of T lymphocytes increases cytoplasmic Ca^{2+} to micromolar levels. During periods of Ca^{2+} entry through CRAC channels, T lymphocytes could become depolarized because of the inward current carried by Ca^{2+} ions. This in turn would lead to the dissipation of the electrochemical gradient required for continued Ca^{2+} entry. In resting human T cells that express ~400 *Kv1.3* channels along with only ~10 *IKCa1* channels and ~10 CRAC channels (9), the K_V channels should be sufficient to compensate for transient depolarization by opening to allow K^+ efflux, resulting in repolarization of the cell. Indeed, high K^+ extracellular solution or blockade of these channels by ChTX, correolide, ShK-Dap[22], or organic antagonists such as progesterone suppresses mitogenesis and IL-2 production (20, 39, 43–46). In each case, depolarization of the membrane potential resulting from K^+ channel block or manipulation of K^+ gradients limits Ca^{2+} entry.

The situation is significantly different in Jurkat T cells and in previously activated human T lymphocytes, both containing roughly equivalent numbers of K_{Ca} (~300–500/cell) and K_V (300–600/cell) channels (10). It is likely that the increased number of CRAC channels in these cells (~100–300/cell) (9) overpowers the ability of *Kv1.3* channels to maintain membrane potential, as evidenced by the fact that K_V channel blockers can no longer suppress proliferation (38, 39). The up-regulation of K_{Ca} channel expression during T cell activation is sufficient to compensate for increased Ca^{2+} influx, because T cells have been observed to hyperpolarize during sustained Ca^{2+} signaling (47). Conversely, T cells depolarize during blockade of K_{Ca} channels, resulting in reduced Ca^{2+} entry and emphasizing the importance of K_{Ca} channels in maintaining the membrane potential (Fig. 2, *A* and *C*) (48, 49). This interplay between channel activation and changes in the membrane potential is likely to result in the repeated depolarization and repolarization that contributes to oscillatory Ca^{2+} entry (21, 50, 51).

Are the roles of the different K_{Ca} channels found in T lymphocytes and in Jurkat cells interchangeable? Both channels are activated by the same mechanism, the binding of Ca^{2+} to calmodulin preassociated with the cytoplasmic C terminus of the channel (29, 37, 38). Both open in response to small changes in intracellular Ca^{2+} concentrations, providing the counterbalancing cation efflux and maintaining the membrane potential required for long lasting Ca^{2+} entry. Indeed, *IKCa1* can effectively substitute for blocked Jurkat *SKCa2* (Fig. 5). Thus, the K_{Ca} channels in Jurkat cells (*SKCa2*) and in activated human T lymphocytes (*IKCa1*) seem to play identical roles in Jurkat T cells and in activated T lymphocytes.

The sustained Ca^{2+} response of T lymphocytes is necessary for maintenance of nuclear factor of activated T cells in the nucleus and for numerous other events in T cell activation (4, 6). We are now beginning to understand the critical role played by K_{Ca} channels in this signaling cascade. In human T cells, K_{Ca} channel blockers prevent T cell proliferation and may become therapeutically useful (38, 40, 52). In Jurkat cells, selective inhibition by UCL 1684 of IL-8 production over IL-2 production (see under "Results") hints that reduction of Ca^{2+} entry may have complex effects on cytokine gene expression. Indeed, the reduced Ca^{2+} entry observed in Th2 cells compared with Th1 cells results in part from the lower level of K_{Ca} channel expression in Th2 cells (30). Future work should help to clarify the role that these channels play in cytokine expression and in determining the cytokine profile of T cells during differentiation.

Acknowledgments—We thank Dr. Luette Forrest for expert technical assistance, Stephan Grissmer for help in early work on the UCL compounds, and C. T. Fun, Dr. D. Yang, and L. Arifhodzic for assistance with strategy and compound synthesis.

REFERENCES

1. Flanagan, W. M., Corthésy, B., Bram, R. J., and Crabtree, G. R. (1991) *Nature* **352,** 803–807
2. Northrop, J. P., Ullman, K. S., and Crabtree, G. R. (1993) *J. Biol. Chem.* **268,** 2917–2923
3. Monks, C. R. F., Freiberg, B. A., Kupfer, H., Sciaky, N., and Kupfer, A. (1998) *Nature* **395,** 82–86
4. Acuto, O., and Cantrell, D. (2000) *Annu. Rev. Immunol.* **18,** 167–184
5. Rao, A., Luo, C., and Hogan, P. G. (1997) *Annu. Rev. Immunol.* **15,** 707–747
6. Crabtree, G. R. (1999) *Cell* **96,** 611–614
7. Zweifach, A., and Lewis, R. S. (1993) *Proc. Natl. Acad. Sci. U. S. A.* **90,** 6295–6299
8. Partiseti, M., Le Deist, F., Hivroz, C., Fischer, A., Korn, H., and Choquet, D. (1994) *J. Biol. Chem.* **269,** 32327–32335
9. Fomina, A. F., Fanger, C. M., Kozak, J. A., and Cahalan, M. D. (2000) *J. Cell Biol.* **150,** 1435–1444
10. Lewis, R. S., and Cahalan, M. D. (1995) *Annu. Rev. Immunol.* **13,** 623–653
11. Grissmer, S., Lewis, R. S., and Cahalan, M. D. (1992) *J. Gen. Physiol.* **99,** 63–84
12. Grissmer, S., Nguyen, A. N., Aiyar, J., Hanson, D. C., Mather, R. J., Gutman, G. A., Karmilowicz, M. J., Auperin, D. D., and Chandy, K. G. (1994) *Mol. Pharmacol.* **45,** 1227–1234
13. Jäger, H., Adelman, J. P., and Grissmer, S. (2000) *FEBS Lett.* **469,** 196–202
14. Desai, R., Peretz, A., Idelson, H., Lazarovici, P., and Attali, B. (2000) *J. Biol. Chem.* **275,** 39954–39963
15. Grissmer, S., Nguyen, A. N., and Cahalan, M. D. (1993) *J. Gen. Physiol.* **102,** 601–630
16. Ishii, T. M., Silvia, C., Hirschberg, B., Bond, C. T., Adelman, J. P., and Maylie, J. (1997) *Proc. Natl. Acad. Sci. U. S. A.* **94,** 11651–11656
17. Logsdon, N. J., Kang, J. S., Togo, J. A., Christian, E. P., and Aiyar, J. (1997) *J. Biol. Chem.* **272,** 32723–32726
18. Joiner, W. J., Wang, L. Y., Tang, M. D., and Kaczmarek, L. K. (1997) *Proc. Natl. Acad. Sci. U. S. A.* **94,** 11013–11018
19. Gelfand, E. W., and Or, R. (1991) *J. Immunol.* **147,** 3452–3458
20. Freedman, B. D., Price, M. A., and Deutsch, C. J. (1992) *J. Immunol.* **149,** 3784–3794
21. Hess, S. D., Oortgiesen, M., and Cahalan, M. D. (1993) *J. Immunol.* **150,** 2620–2633
22. Campos Rosa, J., Dunn, P. M., Galanakis, D., Ganellin, C. R., Yang, D., and Chen, J. Q. (1997) PCT Int. Appl. WO 97/48705
23. Benton, D. C., Roxburgh, C. J., Ganellin, C. R., Shiner, M. A., and Jenkinson, D. H. (1999) *Br. J. Pharmacol.* **126,** 169–178
24. Campos Rosa, J., Galanakis, D., Piergentili, A., Bhandari, K., Ganellin, C. R., Dunn, P. M., and Jenkinson, D. H. (2000) *J. Med. Chem.* **43,** 420–431
25. Chen, J. Q., Galanakis, D., Ganellin, C. R., Dunn, P. M., and Jenkinson, D. H. (2000) *J. Med. Chem.* **43,** 3478–3481
26. Peter, W., Mitrovic, N., Schiebe, M., Lehmann-Horn, F., and Lerche, H. (1999) *J. Physiol. (Lond.)* **518,** 13–22
27. Stefani, E., Ottolia, M., Noceti, F., Olcese, R., Wallner, M., Latorre, R., and Toro, L. (1997) *Proc. Natl. Acad. Sci. U. S. A.* **94,** 5427–5431
28. Rauer, H., Lanigan, M. D., Pennington, M. W., Aiyar, J., Ghanshani, S., Cahalan, M. D., Norton, R. S., and Chandy, K. G. (2000) *J. Biol. Chem.* **275,** 1201–1208
29. Fanger, C. M., Ghanshani, S., Logsdon, N. J., Rauer, H., Kalman, K., Zhou, J., Beckingham, K., Chandy, K. G., Cahalan, M. D., and Aiyar, J. (1999) *J. Biol. Chem.* **274,** 5746–5754
30. Fanger, C. M., Neben, A. L., and Cahalan, M. D. (2000) *J. Immunol.* **164,** 1153–1160

31. Kalman, K., Pennington, M. W., Lanigan, M. D., Nguyen, A., Rauer, H., Mahnir, V., Paschetto, K., Kem, W. R., Grissmer, S., Gutman, G. A., Christian, E. P., Cahalan, M. D., Norton, R. S., and Chandy, K. G. (1998) *J. Biol. Chem.* **273,** 32697–32707
32. Grissmer, S., Dethlefs, B., Wasmuth, J. J., Goldin, A. L., Gutman, G. A., Cahalan, M. D., and Chandy, K. G. (1990) *Proc. Natl. Acad. Sci. U. S. A.* **87,** 9411–9415
33. Campos Rosa, J., Galanakis, D., Ganellin, C. R., Dunn, P. M., and Jenkinson, D. H. (1998) *J. Med. Chem.* **41,** 2–5
34. Thastrup, O., Cullen, P. J., Drobak, B. K., Hanley, M. R., and Dawson, A. P. (1990) *Proc. Natl. Acad. Sci. U. S. A.* **87,** 2466–2470
35. Fanger, C. M., Hoth, M., Crabtree, G. R., and Lewis, R. S. (1995) *J. Cell Biol.* **131,** 655–667
36. Cai, Y., Osbourne, P., North, R., Dooley, D., and Douglass, J. (1992) **11,** 163–172
37. Xia, X. M., Fakler, B., Rivard, A., Wayman, G., Johnson-Pais, T., Keen, J. E., Ishii, T., Hirschberg, B., Bond, C. T., Lutsenko, S., Maylie, J., and Adelman, J. P. (1998) *Nature* **395,** 503–507
38. Khanna, R., Chang, M. C., Joiner, W. J., Kaczmarek, L. K., and Schlichter, L. C. (1999) *J. Biol. Chem.* **274,** 14838–14849
39. Ghanshani, S., Wulff, H., Miller, M. J., Rohm, H., Neben, A., Gutman, G. A., Cahalan, M. D., and Chandy, K. G. (2000) *J. Biol. Chem.* **275,** 37137–37149
40. Wulff, H., Miller, M. J., Hansel, W., Grissmer, S., Cahalan, M. D., and Chandy, K. G. (2000) *Proc. Natl. Acad. Sci. U. S. A.* **97,** 8151–8156
41. Tu, L., Santarelli, V., and Deutsch, C. (1995) *Biophys. J.* **68,** 147–156
42. Ishii, T. M., Maylie, J., and Adelman, J. P. (1997) *J. Biol. Chem.* **272,** 23195–23200
43. Chandy, K. G., DeCoursey, T. E., Cahalan, M. D., McLaughlin, C., and Gupta, S. (1984) *J. Exp. Med.* **160,** 369–385
44. Price, M., Lee, S. C., and Deutsch, C. (1989) *Proc. Natl. Acad. Sci. U. S. A.* **86,** 10171–10175
45. Koo, G. C., Blake, J. T., Shah, K., Staruch, M. J., Dumont, F., Wunderler, D., Sanchez, M., McManus, O. B., Sirotina-Meisher, A., Fischer, P., Boltz, R. C., Goetz, M. A., Baker, R., Bao, J. M., Kayser, F., Rupprecht, K. M., Parsons, W. H., Tong, X. C., Ita, I. E., Pivnichny, J., Vincent, S., Cunningham, P., Hora, D., Feeney, W., Kaczorowski, G., and Springer, M. S. (1999) *Cell Immunol.* **197,** 99–107
46. Ehring, G. R., Kerschbaum, H. H., Eder, C., Neben, A. L., Fanger, C. M., Khoury, R. M., Negulescu, P. A., and Cahalan, M. D. (1998) *J. Exp. Med.* **188,** 1593–1602
47. Verheugen, J. A., Vijverberg, H. P., Oortgiesen, M., and Cahalan, M. D. (1995) *J. Gen. Physiol.* **105,** 765–794
48. Verheugen, J. A., Le Deist, F., Devignot, V., and Korn, H. (1997) *Cell Calcium* **21,** 1–17
49. Verheugen, J. A., and Korn, H. (1997) *J. Physiol. (Lond.)* **503,** 317–331
50. Verheugen, J. A., and Vijverberg, H. P. (1995) *Cell Calcium* **17,** 287–300
51. Mason, M. J., Limberis, J., and Schofield, G. G. (1999) *J. Biol. Chem.* **170,** 79–87
52. Jensen, B. S., Odum, N., Jorgensen, N. K., Christophersen, P., and Olesen, S. P. (1999) *J. Biol. Chem.* **96,** 10917–10921